Osteoarthritis and Cartilage 21 (2013) 574–581

Osteoarthritis and Cartilage

Spatial and temporal changes of subchondral bone proceed to microscopic articular cartilage degeneration in guinea pigs with spontaneous osteoarthritis

T. Wang †[a], C.-Y. Wen †[a], C.-H. Yan †, W.-W. Lu †‡, K.-Y. Chiu †*

† Department of Orthopaedics and Traumatology, Li Ka Shing Faculty of Medicine, The University of Hong Kong, Pokfulam, Hong Kong
‡ Research Center for Human Tissues and Organs Degeneration, Shenzhen Institute of Advanced Technology, Chinese Academy of Science, Shenzhen, China

ARTICLE INFO

Article history:
Received 30 August 2012
Accepted 1 January 2013

Keywords:
Early stage osteoarthritis
Guinea pig
Subchondral bone
Ultrastructure

SUMMARY

Objective: This study aimed to investigate the spatial and temporal subchondral bone change of Dunkin–Hartley (DH) strain guinea pigs spontaneous osteoarthritis (OA) model at early stage with three-dimensional Microfocal Computed Tomography (Micro-CT) analysis, histology and immunohistochemistry.
Materials and methods: Knee joints of DH and Bristol Strain 2 (BS2) guinea pigs were analyzed at 1, 2 and 3 months of age for early staged subchondral bone ultrastructure change of OA by Micro-CT and histology. And cartilage degeneration was monitored by histological examination. In addition, expression of Osterix was quantified by immunohistochemistry.
Results: Microscopic cartilage degeneration was not found at first 3 months in both DH and BS2 guinea pigs. Subchondral bone sclerosis with trabecular ultrastructure turnover was characterized in subchondral bone of DH guinea pigs. Increased thickness, bone mineral density with decreased porosity were defined in subchondral plate of DH guinea pigs. Subchondral trabecular bone was found to be plate-like, convex and isotropy with higher bone volume. Histology confirmed the finding of lower porosity at osteochondral junction and increased bone volume. Immunohistochemistry revealed that the early OA subchondral bone change may be due to elevated level of osteoblast differentiation.
Conclusions: Subchondral bone ultrastructure change occurred at early stage of OA ahead of microscopic cartilage degeneration, which may further impair articular cartilage. It was possibly related to elevated level of osteoblast differentiation.

Introduction

Osteoarthritis (OA) is one of the most prevalent joint disorders which bring enormous challenge to social economics. Nowadays, early OA changes have drawn attention and it has been postulated that osteochondral changes occur early during the development of OA and may aggravate pathology elsewhere in the joint[1].

Recently, subchondral bone change was reported to play an important role in OA pathogenesis and attracted more and more attention[2–5]. Change in organization and composition of subchondral bone may lead to altered mechanical property, which makes the bone "brittle", adversely affecting the overlying articular cartilage[5]. Invasion of vascular elements at tidemark may result in advancement of the calcified cartilage into the deep zones of the articular cartilage, leading to local cartilage thinning[6]. Besides, turnover of subchondral bone remodeling may give rise to the formation of osteophytes[7]. Additionally, early subchondral bone turnover at osteochondral junction during the development of OA may impair molecule crosstalk between cartilage and bone and aggravate OA. However, the exact subchondral bone change is still unknown, especially at early stage of OA.

Dunkin–Hartley (DH) strain guinea pig is a well-established and widely used OA model. It has been reported that in DH guinea pig OA model, the number of chondrocytes was diffusely decreased in the tangential zone, and proteoglycan loss was observed at 5 months[2]. Up to now, the early subchondral bone change on OA initiation is still poorly understood. Janet studied subchondral bone mineral density (BMD) at age of 3, 6, 9 and 12 weeks and reported

* Address correspondence and reprint requests to: K.-Y. Chiu, Room 216, New Clinical Building, Queen Mary Hospital, Pokfulam, Hong Kong. Tel: 852-2255-4654; Fax: 852-2817-4392.
E-mail addresses: wang_ting@hku.hk (T. Wang), paulwen@hku.hk (C.-Y. Wen), yanchunhoi@gmail.com (C.-H. Yan), wwlu@hku.hk (W.-W. Lu), pkychiu@hku.hk (K.-Y. Chiu).
[a] They equally contributed to this study.

1063-4584/$ – see front matter
http://dx.doi.org/10.1016/j.joca.2013.01.002

DH have significantly lower bone density than Bristol Strain 2 (BS2) at 9 weeks[8]. However, the result of that study was based on plain X-ray with low image quality. The spatial change in subchondral bone is still not clear. In this study, we investigated the spatial and temporal subchondral bone change of DH guinea pig spontaneous OA model at early stage of OA initiation comparing with BS2 guinea pigs as OA-free control[9,10].

Material and methods

Animals

The Committee On The Use Of Live Animals In Teaching & Research of authors' institute approved all the protocols and procedures in this study. Six animals from each strain were sacrificed at ages 1, 2 and 3 months with intraperitoneally injection of 100 mg/kg pentobarbital. The bilateral knee joints were excised. One knee joint was used for the Microfocal Computed Tomography (Micro-CT) scan and analysis, and the other one was used for histopathologic evaluation.

Micro-CT study

Knee joints were scanned and analyzed using SkyScan 1076 Micro-CT system and softwares (SkyScan, Kontich, Belgium) with voxel size 18 μm, voltage 100 kV, exposure time 2356 ms, frame averaging 2, beam filtration filter 1.0 mm aluminum. After scanning, knee joint was three-dimensionally reconstructed by *SkyScan recon* software. For analysis of subchondral plate, the load-bearing region with an area of 1.04×1.04 mm^2 was selected as Region of Interest (ROI). BMD, porosity, and thickness of subchondral plate were measured and calculated using *CT-analyser* software. For analysis of subchondral trabecular bone, a cuboid of trabecular bone with size of $1.04 \times 1.04 \times 0.52$ mm^3 at beneath the ROI of subchondral plate was selected. BMD (g/cm^3), percent bone volume (BV/TV, %), trabecular thickness (TbTh, mm), trabecular separation (Tb.Sp, mm), trabecular bone pattern factor (TbPf, 1/mm), structure model index (SMI), and degree of anisotropy (DA) were calculated for subchondral trabecular bone. Additionally, joint space was also measured by *CT-analyser* with well-established protocol[11].

Histological analysis

Knee joints of both DH and BS2 guinea pigs were harvested and fixed in 10% neutral buffered formalin solution for 3 days and decalcified at 4°C for 4–5 weeks with 0.5 M ethylenediaminetetraacetic acid (EDTA). The sample was dehydrated and embedded in paraffin by the standard method. Twenty serial sections were prepared from the central region of the medial tibial plateau in the sagittal plane at 5–7 μm and alternately stained with Hematoxylin and Eosin (H&E) and Toluidine blue. Images were captured using Nikon H600L Microscope (Japan). Slides stained with Toluidine blue were evaluated with Modified Mankin score in three histologic sections per joint[12]. Meanwhile, ratio of pore area/total area at osteochondral junction and bone area/total area of subchondral trabecular bone was quantified by Image-Pro Plus version 5.0 (Media Cybernetics, Inc. USA) on H&E stained slides to analyze the ultrastructure of subchondral plate and subchondral trabecular bone.

Immunohistochemistry

Sections were deparaffinized in xylene and rehydrated in grade alcohol, and quenched in 0.3% hydrogen peroxide in methanol. Then slides were blocked in 5% goat serum (Invitrogen, USA) and incubated overnight in a humid chamber at 4°C in primary antibody rabbit IgG clone of Osterix (Abcam, UK). On the second day, the sections were incubated in secondary antibody of Rabbit ExtrAvidin Peroxidase Staining Kit (Sigma–Aldrich, USA) and visualized by reaction with 3,3′-diaminobenzidine (DAB) substrate (SK-4100, Vector Laboratories). Images were captured using Nikon H600L Microscope (Japan). The number of Osterix positive stained cells was quantified with Image-Pro Plus version 5.0. At least three sections from three samples for each time point of each strain were measured for analysis. For each section, three areas were analyzed, corresponding to anterior, center and posterior portions of the tibial subchondral bone. The mean of the three portions and three sections was taken as the value for the animal.

Statistical analysis

We used R version 2.11.1 analysis software (Lucent Technologies, France) in all statistical analyses. Since the sample size is small ($n = 6$), non-parametric statistical analysis Wilcoxon test was performed for comparison between DH and BS2. A P value <0.05 was considered to be significant. For comparison of ultrastructure properties among medial and lateral sides of DH and BS2 strain, *post-hoc* multiple comparisons between groups were made using the Kruskal–Wallis test. When significant main effects were found, Wilcoxon tests with Bonferroni correction were carried out to compare the DH and BS2 groups determined between-subjects factor, as well as the medial and lateral groups determined within-subjects factor. Bonferroni correction was used to control familywise error rate due to multiple hypotheses tests. And one-sided Wilcoxon tests were performed within groups to investigate the temporal change with groups.

Results

Cartilage degeneration was not detected by Modified Mankin score in either strain of guinea pig

From the result of Toluidine blue staining, cartilage damage was not obviously observed by age of 3 months [Fig. 1(a)] in either strains. There is no significant difference of Modified Mankin score between two strains [Fig. 1(c)]. However, early sign of OA was observed in term of joint space narrowing (JSN) at 1 (0.73 ± 0.09 mm for BS2 and 0.48 ± 0.05 mm for DH, $P = 0.002$) and 2 months [0.52 ± 0.07 mm for BS2 and 0.31 ± 0.05 mm for DH, $P = 0.002$, Fig. 1(d)].

Subchondral plate: higher BMD, thickness and lower porosity in DH group

ROI was shown in Fig. 2(a). BMD of the medial tibial subchondral plate was significantly higher in DH guinea pigs than in BS2 guinea pigs at age of 2 (0.776 ± 0.069 g/cm^3 for BS2 and 0.998 ± 0.085 g/cm^3 for DH, $P = 0.002$) and 3 months [0.956 ± 0.090 g/cm^3 for BS2 and 1.238 ± 0.121 g/cm^3 for DH, $P = 0.002$, Fig. 2(b)]. In DH guinea pigs, BMD increased significantly from age 2–3 months (0.998 ± 0.085 g/cm^3 for 2 months and 1.238 ± 0.121 g/cm^3 for 3 months, $P = 0.002$). In contrast, BMD was not significantly increased temporally in BS2. Subchondral plate thickness was significantly higher in DH guinea pigs than BS2 at age 1 (0.237 ± 0.039 mm for BS2 and 0.346 ± 0.052 mm for DH, $P = 0.002$), 2 (0.290 ± 0.040 mm for BS2 and 0.427 ± 0.048 mm for DH, $P = 0.002$) and 3 months [0.365 ± 0.049 mm for BS2 and 0.528 ± 0.053 mm for DH, $P = 0.002$, Fig. 2(c)].

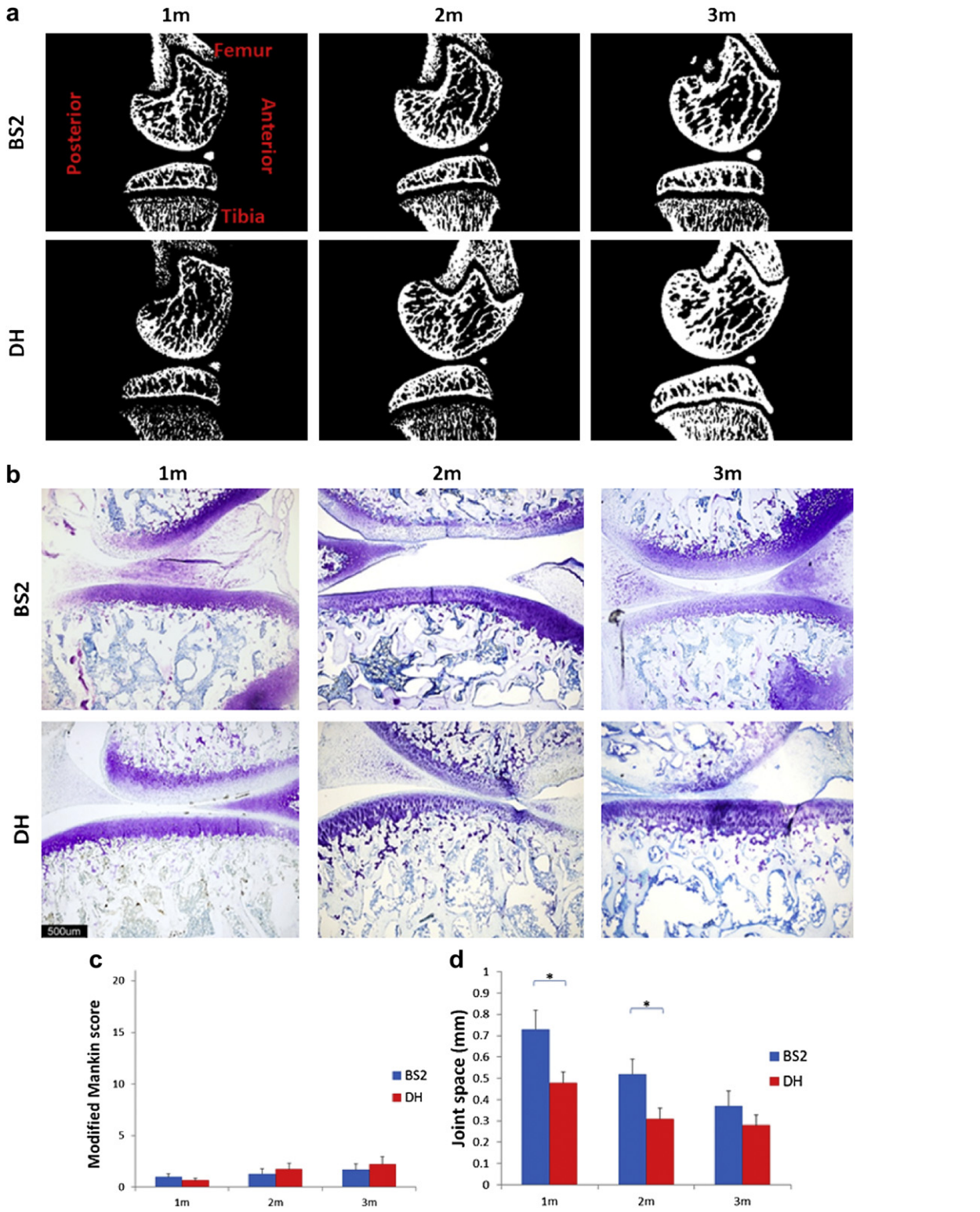

Fig. 1. (a) Demographic Micro-CT image showed narrowed joint space of DH strain guinea pigs at age of 1 and 2 months; (b) Overall view of knee joint histology with Toluidine blue staining of DH and BS2 strain guinea pigs. Obvious cartilage destruction was observed in neither strain; (c) Modified Mankin score showed no significant difference in joint degeneration between BS2 and DH strain guinea pigs at 1, 2 and 3 months; (d) Quantitative analysis showed the joint space in DH strain guinea pig was significantly narrower than BS2 at 1 and 2 months.

Significant lower porosity was defined in medial subchondral plate of DH guinea pig than BS2 at age of 1 (32.76 ± 3.5% for BS2 and 20.53 ± 2.7% for DH, $P = 0.002$), 2 (27.43 ± 2.21% for BS2 and 14.72 ± 1.8% for DH, $P = 0.002$) and 3 months [19.27 ± 2.3% for BS2 and 7.55 ± 1.1% for DH, $P = 0.002$, Fig. 2(d)]. In DH group, porosity of medial subchondral plate was significantly lower than lateral side at age of 2 ($P = 0.002$) and 3 months ($P = 0.002$). However, such difference was not observed in BS2. Porosity decreased in both medial

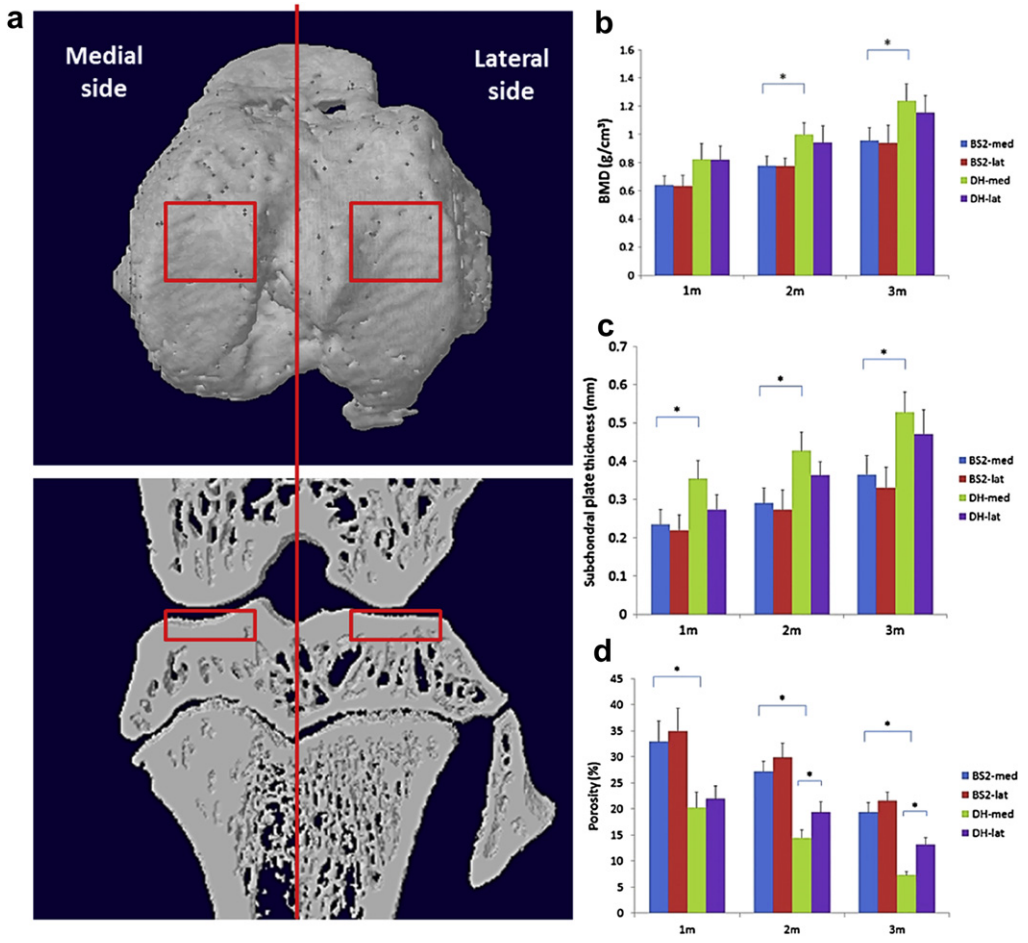

Fig. 2. Micro-CT analysis of tibia subchondral plate. (a) Demographic images of top and coronal views of ROI selection of medial and lateral tibia subchondral plate for analysis of subchondral plate BMD, thickness and porosity; (b) Quantitative analysis of BMD showed significant difference between DH and BS2 strain on medial sides at age of 2 and 3 months; (c) Quantitative analysis of subchondral plate thickness showed significant difference between DH and BS2 strain on medial sides at age of 1, 2 and 3 months; (d) Quantitative analysis of subchondral plate porosity showed significant difference between DH and BS2 strain on medial sides at age of 1, 2 and 3 months, while within DH group, significant difference was defined between medial and lateral sides at age of 2 and 3 months.

and lateral sides at age of 2 and 3 months in both strains. In BS2 group, decrease in porosity was 41% in medial side at 3 months comparing with 1 month, while in DH group such decrease was 63%.

Subchondral trabecular bone: higher BV/TV, plate-like, convex and isotropy in DH group

ROI was shown in Fig. 3(a). Significant changes in the microstructure of medial cancellous bone in OA were observed. Compared with normal medial control, it is plate-like, convex, and isotropy in trabecular organization with higher BV/TV.

Results of Micro-CT analysis on 3D ultrastructure parameters of subchondral trabecular bone were summarized in Table I. Significant increase in BMD was observed in DH strain from age 2–3 months in both medial ($P = 0.001$) and lateral sides ($P = 0.002$). While such significant increase in BMD was only observed in BS2 strain at lateral side ($P = 0.008$). BV/TV was higher in medial subchondral trabecular bone of DH group at 1, 2 and 3 months compared with BS2. Within DH group, BV/TV was significantly higher in medial side than lateral at 2 and 3 months, while such significant temporal increase in BV/TV was only observed in BS2 group at 3 months. Significant increase in BV/TV in DH strain was observed at age of 2 ($P = 0.021$) and 3 ($P = 0.002$) months in medial side, as well as 3 months ($P = 0.008$) in lateral sides. Meanwhile in BS2 group, such increase was recorded at age of 3 months ($P = 0.001$) at medial side, as well as 2 ($P = 0.004$) and 3 ($P = 0.002$) months at lateral side. TbTh was greater in DH group than in the BS2 group at age of 3 months ($P = 0.002$). TbTh increased in DH strain at age of 3 months in both medial ($P = 0.002$) and lateral ($P = 0.012$) sides, while such change was not observed in BS2 strain. Tb.Sp was lower in DH group than BS2 group at age of 1 and 2 months.

Trabecular SMI and TbPf were significantly lower in DH guinea pigs than in BS2 guinea pigs at age 1, 2 and 3 months. Difference between medial and lateral sides was significant in DH strain at age of 1, 2 and 3 months of TbPf as well as 2 and 3 months of SMI. While such difference was only observed in BS2 strain at age of 3 months. SMI decreased in DH strain at age of 3 months in both medial ($P = 0.001$) and lateral ($P = 0.021$) sides. Significant change was not observed in BS2 temporally. TbPf decreased in DH strain at age of 2 months in medial side ($P = 0.001$) and 3 months in lateral side ($P = 0.004$). And such decreased was observed in BS2 strain at age of 2 ($P = 0.001$) and 3 ($P = 0.001$) months in medial side as well as 2 months ($P = 0.001$) in lateral side. DA was lower in DH guinea pigs than BS2 at age of 1 and 3 months. And significant lower DA was defined at medial side of subchondral trabecular bone than the lateral side at age of 1, 2 and 3 months for DH strain and 2 and 3 months for BS2. In DH group, DA decreased at 3 months in both medial ($P = 0.001$) and lateral sides ($P = 0.008$). In BS2 group, DA

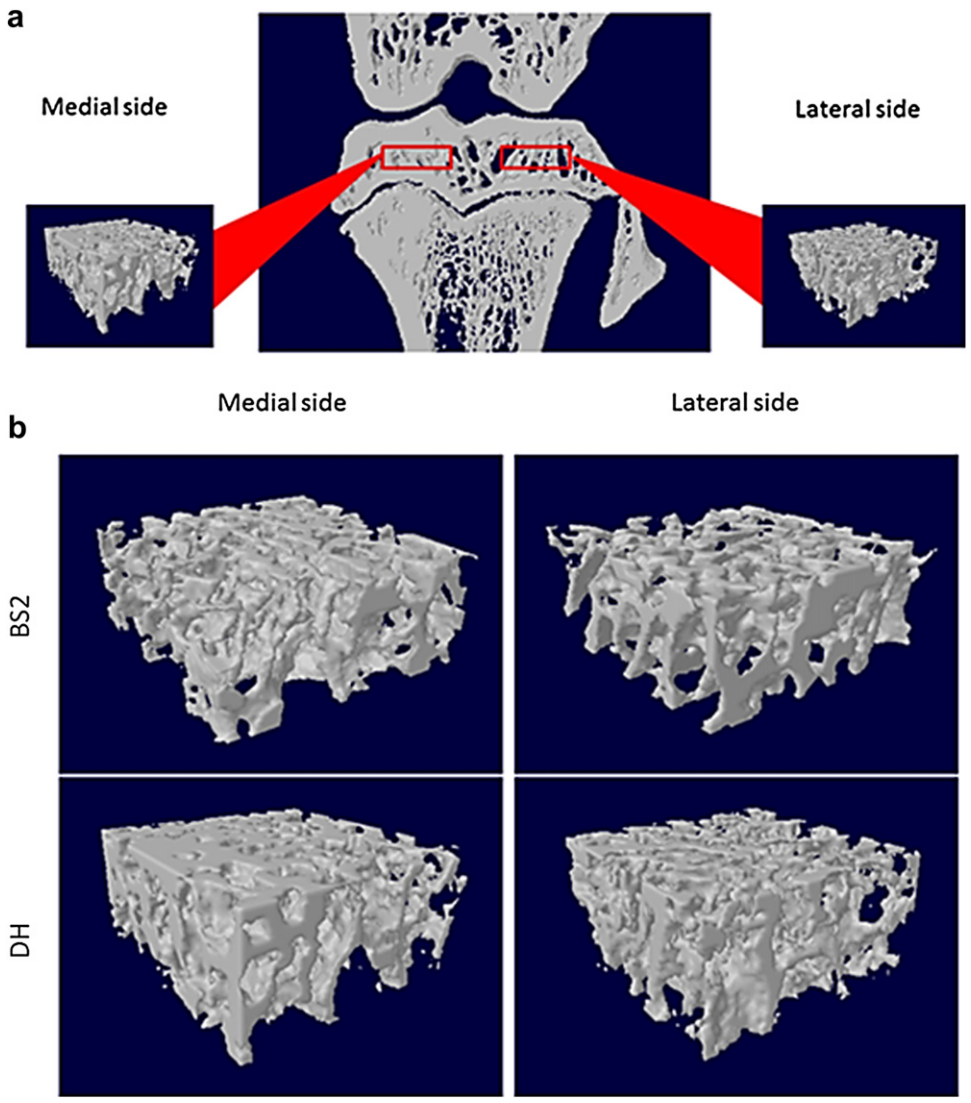

Fig. 3. Micro-CT analysis of tibia subchondral trabecular bone. (a) ROI selection of medial and lateral tibia subchondral trabecular bone; (b) Diaphragmatic image of medial and lateral tibia subchondral trabecular bone of DH and BS2 guinea pig at age of 3 months.

decreased at 2 months in only medial side ($P = 0.001$), but increased at 3 months in both medial ($P = 0.004$) and lateral sides ($P = 0.002$).

Histological findings: less porous and higher trabecular area in DH group

DH group is lower in pore area/total area ratio at age of 1 (13.7 ± 2.52% for BS2 and 8.4 ± 1.3% for DH, $P = 0.004$) and 3 months [8.9 ± 1.4% for BS2 and 6.2 ± 1.1% for DH, $P = 0.009$, Fig. 4(b)] and higher in ratio of trabecular area/total area at 1 month [53.3 ± 6.1% for BS2 and 76.4 ± 7.9% for DH, $P = 0.002$, Fig. 4(c)]. The histological finding showed that DH guinea pigs have less pores in subchondral plate and higher bone volume in subchondral trabecular bone, which was in accordance with the finding of Micro-CT.

Immunohistochemistry: larger number of Osterix positive stained cells in DH group

In this study of immunohistochemistry, significant larger number of Osterix positive stained cells was observed in DH group than BS2 group at age of 1 (11 ± 3.3 for BS2 and 27 ± 2.4 for DH, $P = 0.005$), 2 (19 ± 2.9 for BS2 and 29 ± 2.6 for DH, $P = 0.005$) and 3 months [22 ± 2.6 for BS2 and 33 ± 2.6 for DH, $P = 0.002$, Fig. 5(b)]. This finding suggested elevated level of osteoblast differentiation in DH guinea pigs subchondral bone than that of BS2.

Discussion

DH strain guinea pig is a well-established spontaneous OA model which manifests degeneration of cartilage, bone and the whole joint. Cartilage degeneration was observed at 5 months of age with fibrillation and proteoglycan loss[2]. In this study, significant cartilage degeneration was not identified at microscopic level by age of 3 months in both strains. Meanwhile spatial and temporal ultrastructure changes in subchondral bone were defined by Micro-CT in DH strain with denser, thicker and less porous subchondral plate and plate-like, convex and isotropic subchondral trabecular bone. Therefore, the finding of this study suggested that subchondral bone change at early stage of OA may proceed to microscopic cartilage damage at later stage.

JSN was observed at 1 and 2 months in DH strain without lesion of cartilage destruction. It has been reported that besides cartilage

Table I
Quantitative Micro-CT analysis of subchondral trabecular bone ($n = 6$)

		BS2-med		BS2-lat		*P* value (BS2-med vs BS2-lat)	DH-med		DH-lat		*P* value (DH-med vs DH-lat)	*P* value (DH-med vs BS2-med)
		Mean	SD	Mean	SD		Mean	SD	Mean	SD		
BMD (g/cm^3)	1 m	0.583	0.056	0.583	0.071	0.873	0.608	0.061	0.595	0.061	0.937	0.748
	2 m	0.62	0.051	0.613	0.05	0.937	0.649	0.05	0.62	0.055	0.310	0.394
	3 m	0.706	0.082	0.709↑	0.061	1.0	0.83↑	0.057	0.776↑	0.056	0.093	0.015
BV/TV (%)	1 m	27.45	3.56	22.01	3.13	0.065	47.00	3.39	40.69	5.17	0.041	0.002
	2 m	30.36	4.45	27.03↑	1.81	0.240	52.89↑	4.25	41.81	4.93	0.004	0.002
	3 m	45.30↑	3.96	35.29↑	3.71	0.004	66.38↑	5.19	51.44↑	6.66	0.004	0.002
TbTh (mm)	1 m	0.116	0.02	0.106	0.017	0.373	0.140	0.017	0.122	0.017	0.240	0.093
	2 m	0.131	0.026	0.120	0.019	0.485	0.160	0.018	0.133	0.015	0.015	0.078
	3 m	0.166	0.027	0.149	0.019	0.310	0.209↑	0.027	0.170↑	0.025	0.041	0.004
Tb.Sp (mm)	1 m	0.238	0.017	0.272	0.016	0.015	0.176	0.014	0.161	0.013	0.132	0.002
	2 m	0.278↑	0.017	0.289	0.017	0.336	0.165	0.014	0.181↑	0.011	0.065	0.002
	3 m	0.212↓	0.019	0.212↓	0.015	1.0	0.180	0.015	0.206↑	0.015	0.026	0.016
TbPf (1/mm)	1 m	8.79	0.84	10.11	1.1	0.065	−3.19	0.32	−0.42	0.035	0.002	0.002
	2 m	6.52↓	0.77	7.59↓	0.72	0.041	−4.38↓	0.38	−0.39	0.034	0.002	0.002
	3 m	2.51↓	0.18	8.49	0.78	0.002	−4.37	0.4	−0.49↓	0.044	0.005	0.002
SMI	1 m	1.935	0.264	1.897	0.513	0.818	0.926	0.266	1.366	0.215	0.009	0.002
	2 m	1.688	0.308	1.913	0.5	0.394	0.801	0.153	1.505	0.312	0.002	0.002
	3 m	1.629	0.271	2.550	0.418	0.004	0.258↓	0.04	1.007↓	0.262	0.002	0.002
DA	1 m	0.380	0.04	0.311	0.068	0.109	0.242	0.037	0.443	0.052	0.002	0.002
	2 m	0.203↓	0.027	0.353	0.033	0.002	0.256	0.032	0.448	0.048	0.002	0.015
	3 m	0.272↑	0.033	0.470↑	0.043	0.002	0.118↓	0.042	0.370↓	0.034	0.002	0.002

↑: significant increase comparing with previous time point, $P < 0.05$; ↓: significant decrease comparing with previous time point, $P < 0.05$.

damage, JSN is also correlated with knee alignment and biomechanics[13] on OA initiation. OA in DH guinea pig was possibly induced by knee laxity[10]. The malalignment of mechanical load may lead to narrowed joint space and act as a stimulus for subchondral bone and cartilage change. Then the later compensation of subchondral bone and cartilage may alleviate JSN somehow. This may be the possible reason that joint space is similar in both strains at 3 months.

The findings of this study match previously reported data of human research. For instance, Ding *et al.* analyzed human OA subchondral cancellous bone and reported that medial OA cancellous bone was significantly thicker, denser and markedly plate-like, but lower in mechanical properties than normal bone[4]. In another study, Chiba *et al.* reported that trabecular bone thickening and associated structural changes were observed in early and advanced OA[14]. This finding suggested that DH strain guinea pig is a useful model of subchondral bone change in OA. Meanwhile, opposite results were also reported. Sniekers *et al.* reported strongly reduced thickness and increased porosity in subchondral plate in canine groove and Anterior Cruciate Ligament Transection (ACLT) OA models[15]. Similar findings were also reported by Hayami *et al.*[16] and Botter *et al.*[17] It was claimed that increased turnover or remodeling of subchondral bone could produce an increase in subchondral bone resorption which would favor the initiation and could aggravate the development of OA. Herrero-Beaumont *et al.*[18] reviewed previous work and concluded that both high and low BMD conditions may be harmful for cartilage homeostasis and could predispose to OA initiation. An interesting finding was that the DH guinea pig with increased BMD in this study belongs to spontaneous OA model, while the ACLT and groove models manifest decreased BMD is surgically induced. Yet it's not clear whether the extreme BMD condition at OA initiation is correlated with different types of animal models.

In this study subchondral trabecular bone of DH guinea pig was found to change from rod-like to plate-like which is opposite to the normal aging process[19]. Such change may make subchondral bone stiff[20] and harmful to articular cartilage. Meanwhile, lower DA identified in DH strain indicated inferior capability of subchondral cancellous bone to transfer load from cartilage[21]. The changes in ultrastructure and organization was an adaptation to changes in the biomechanics of the joint and an attempt to repair micro-damage. Unfortunately it was accompanied with turnover and made the subchondral bone become brittle and unable to transfer load for cartilage efficiently, which would further impair the overlying articular cartilage[5].

Another controversy with previous reported data is that someone reported increased subchondral plate porosity during the whole process of OA progression[15,17]. In this study, decreased porosity in subchondral plate was observed by Micro-CT analysis, and then confirmed by histology. This is partially due to the rapid growth of animals. However, comparing with BS2, significant higher bone mass and lower porosity were defined in DH strain. Therefore comparing with BS2 strain as the baseline "physiological growth curve", the overgrowth of subchondral bone in DH guinea pig is postulated as one of the predisposing factors for OA initiation. Additionally, together with the finding of immunohistochemistry, it may indicate a mechanism of bone remodeling in early OA. According to Parfitt *et al.*, The elevated TbTh but relatively declined

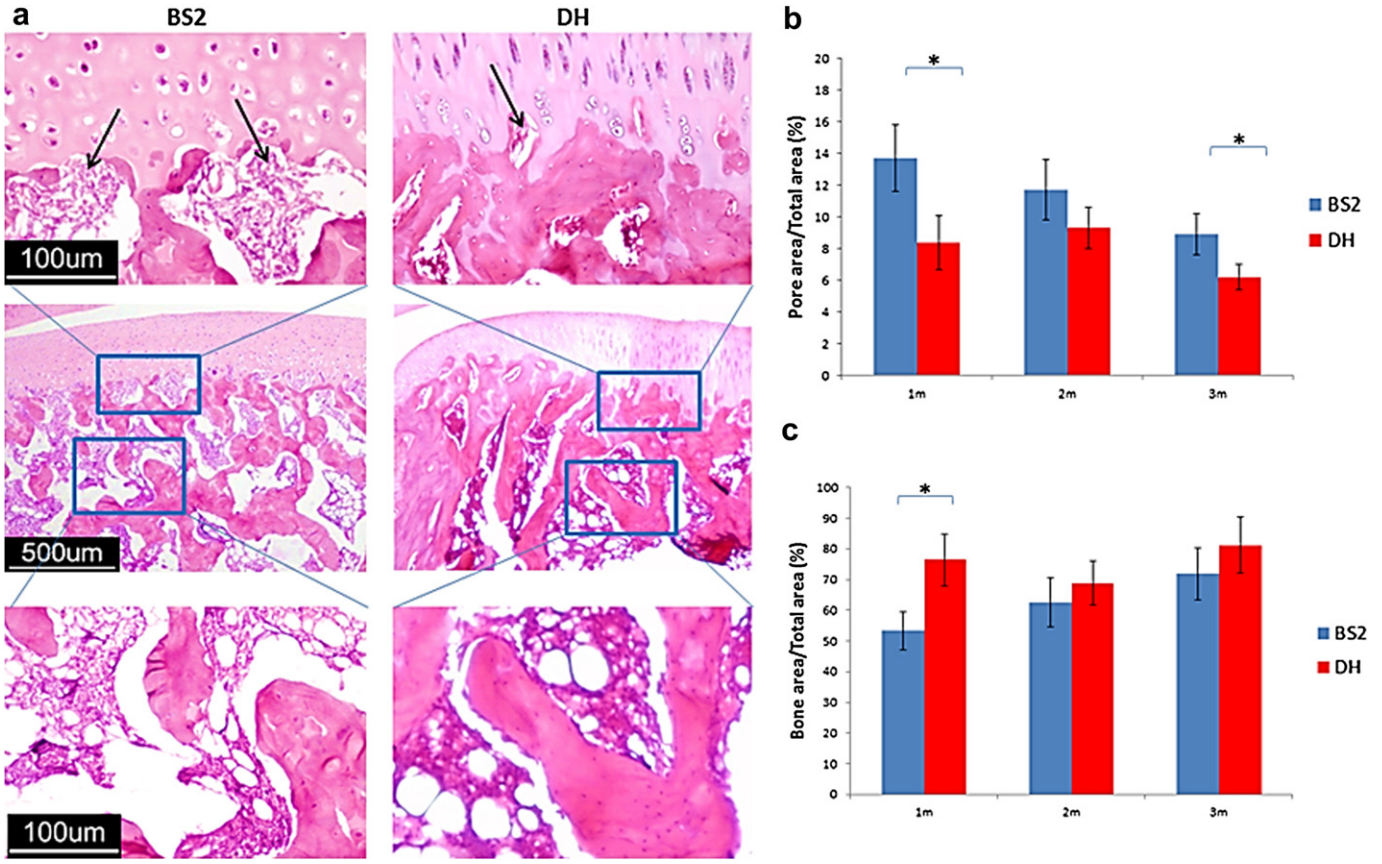

Fig. 4. Diaphragmatic histological image of tibial end of knee joints of BS2 and DH guinea pigs at age of 1 month. (a) Diaphragmatic image of pore area at osteochondral junction (black arrow) and subchondral trabecular bone area of tibial end of knee joints of BS2 and DH guinea pigs at age of 1 month; (b) Quantitative analysis showed significant lower ratio of pore area/total area comparing with BS2 strain at age of 1 and 3 months; (c) Quantitative analysis showed significant higher ratio of bone area/total area comparing with BS2 strain at age of 1 month.

connectivity suggests a process of filling trabecular cavities[22]. This process is possibly some kind of compensation to the biomechanical challenge. However, it may fail to entirely counteract for a total decrease of mechanical properties in early OA[4]. Furthermore, the sclerosis and thickening of subchondral plate may impair the molecule crosstalk between articular cartilage and subchondral bone, which may further impair the catabolism of articular cartilage[23].

In conclusion, subchondral bone changes in early stage of OA of guinea pig spontaneous OA model were characterized in both subchondral plate and trabecular bone. Such change is possibly related to elevated level of osteoblast differentiation, which may further impair articular cartilage biologically and mechanically. The finding of this study may contribute to new insight and understanding of early OA pathogenesis and potential development of specific therapeutics strategies.

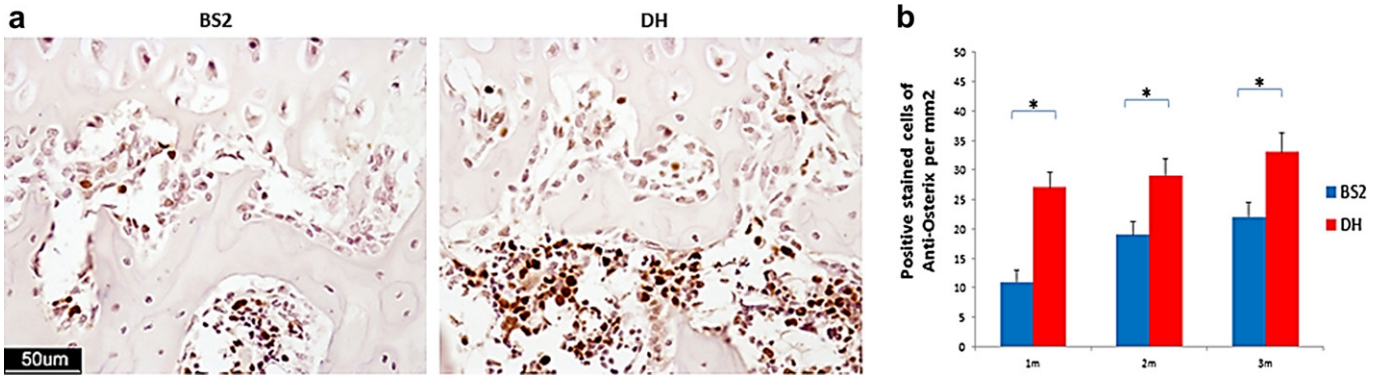

Fig. 5. Immunohistochemistry of anti-Osterix at osteochondral junction of BS2 and DH guinea pigs. (a) Diaphragmatic image showed positive stained cells of BS2 and DH guinea pigs at age of 3 months; (b) Histomorphometry showed significant larger number of positive stained cells of anti-Osterix per mm^2 in DH group than BS2 group at age of 1, 2 and 3 months.

Author contributions

All authors made substantial contributions to study design, analysis and interpretation of data, drafting the manuscript and editing for important intellectual content of this article.

Role of funding source

The study is supported by Li Shu Fan Medical Foundation and partially supported by National Natural Science Foundation of China (NSFC)/ Research Grant Council of The University of Hong Kong 739/10 and NSFC 81270967.

Conflict of interest

The authors acknowledge that there are no conflicts of interest pertaining to this manuscript.

Acknowledgments

The authors would like to thank Miss Yan Wang from Division of Bioinformatics, Department of Biochemistry, The University of Hong Kong for assistance in statistical analysis.

References

1. Suri S, Walsh DA. Osteochondral alterations in osteoarthritis. Bone 2012;51(2):204–11.
2. Muraoka T, Hagino H, Okano T, Enokida M, Teshima R. Role of subchondral bone in osteoarthritis development: a comparative study of two strains of guinea pigs with and without spontaneously occurring osteoarthritis. Arthritis Rheum 2007;56(10):3366–74.
3. Bailey AJ, Mansell JP. Do subchondral bone changes exacerbate or precede articular cartilage destruction in osteoarthritis of the elderly? Gerontology 1997;43(5):296–304.
4. Ding M, Odgaard A, Hvid I. Changes in the three-dimensional microstructure of human tibial cancellous bone in early osteoarthritis. J Bone Joint Surg Br 2003;85(6):906–12.
5. Day JS, Ding M, van der Linden JC, Hvid I, Sumner DR, Weinans H. A decreased subchondral trabecular bone tissue elastic modulus is associated with pre-arthritic cartilage damage. J Orthop Res 2001;19(5):914–8.
6. Walsh DA, Bonnet CS, Turner EL, Wilson D, Situ M, McWilliams DF. Angiogenesis in the synovium and at the osteochondral junction in osteoarthritis. Osteoarthritis Cartilage 2007;15(7):743–51.
7. Cotofana S, Buck R, Wirth W, Roemer F, Duryea J, Nevitt M, *et al*. Cartilage thickening in early radiographic knee osteoarthritis: a within-person, between-knee comparison. Arthritis Care Res (Hoboken) 2012;64(11):1681–90.
8. Anderson-MacKenzie JM, Quasnichka HL, Starr RL, Lewis EJ, Billingham ME, Bailey AJ. Fundamental subchondral bone changes in spontaneous knee osteoarthritis. Int J Biochem Cell Biol 2005;37(1):224–36.
9. Quasnichka HL, Anderson-MacKenzie JM, Bailey AJ. Subchondral bone and ligament changes precede cartilage degradation in guinea pig osteoarthritis. Biorheology 2006;43(3–4):389–97.
10. Quasnichka HL, Anderson-MacKenzie JM, Tarlton JF, Sims TJ, Billingham ME, Bailey AJ. Cruciate ligament laxity and femoral intercondylar notch narrowing in early-stage knee osteoarthritis. Arthritis Rheum 2005;52(10):3100–9.
11. Hellio Le Graverand MP, Mazzuca S, Duryea J, Brett A. Radiographic-based grading methods and radiographic measurement of joint space width in osteoarthritis. Radiol Clin North Am 2009;47(4):567–79.
12. Kraus VB, Huebner JL, DeGroot J, Bendele A. The OARSI histopathology initiative – recommendations for histological assessments of osteoarthritis in the guinea pig. Osteoarthritis Cartilage 2010;18(Suppl 3):S35–52.
13. Vignon E, Brandt KD, Mercier C, Hochberg M, Hunter D, Mazzuca S, *et al*. Alignment of the medial tibial plateau affects the rate of joint space narrowing in the osteoarthritic knee. Osteoarthritis Cartilage 2010;18(11):1436–40.
14. Chiba K, Ito M, Osaki M, Uetani M, Shindo H. In vivo structural analysis of subchondral trabecular bone in osteoarthritis of the hip using multi-detector row CT. Osteoarthritis Cartilage 2011;19(2):180–5.
15. Sniekers YH, Intema F, Lafeber FP, van Osch GJ, van Leeuwen JP, Weinans H, *et al*. A role for subchondral bone changes in the process of osteoarthritis; a micro-CT study of two canine models. BMC Musculoskelet Disord 2008;9:20.
16. Hayami T, Pickarski M, Wesolowski GA, McLane J, Bone A, Destefano J, *et al*. The role of subchondral bone remodeling in osteoarthritis: reduction of cartilage degeneration and prevention of osteophyte formation by alendronate in the rat anterior cruciate ligament transection model. Arthritis Rheum 2004;50(4):1193–206.
17. Botter SM, van Osch GJ, Clockaerts S, Waarsing JH, Weinans H, van Leeuwen JP. Osteoarthritis induction leads to early and temporal subchondral plate porosity in the tibial plateau of mice: an in vivo microfocal computed tomography study. Arthritis Rheum 2011;63(9):2690–9.
18. Herrero-Beaumont G, Roman-Blas JA, Largo R, Berenbaum F, Castaneda S. Bone mineral density and joint cartilage: four clinical settings of a complex relationship in osteoarthritis. Ann Rheum Dis 2011;70(9):1523–5.
19. Ding M, Hvid I. Quantification of age-related changes in the structure model type and trabecular thickness of human tibial cancellous bone. Bone 2000;26(3):291–5.
20. Ding M, Odgaard A, Danielsen CC, Hvid I. Mutual associations among microstructural, physical and mechanical properties of human cancellous bone. J Bone Joint Surg Br 2002;84(6):900–7.
21. Goulet RW, Goldstein SA, Ciarelli MJ, Kuhn JL, Brown MB, Feldkamp LA. The relationship between the structural and orthogonal compressive properties of trabecular bone. J Biomech 1994;27(4):375–89.
22. Parfitt AM, Mathews CH, Villanueva AR, Kleerekoper M, Frame B, Rao DS. Relationships between surface, volume, and thickness of iliac trabecular bone in aging and in osteoporosis. Implications for the microanatomic and cellular mechanisms of bone loss. J Clin Invest 1983;72(4):1396–409.
23. Nakamura T, Mizuno S. The discovery of hepatocyte growth factor (HGF) and its significance for cell biology, life sciences and clinical medicine. Proc Jpn Acad Ser B Phys Biol Sci 2010;86(6):588–610.